ISBN: 978-3-95450-214-1 ISSN: 2673-5490 doi:10.18429/JACoW-IPAC2021-MOPAB416

BDSIM DEVELOPMENTS FOR HADRON THERAPY CENTRE APPLICATIONS

E. Ramoisiaux*, C. Hernalsteens[1], R. Tesse, E. Gnacadja,
M. Vanwelde, N. Pauly, Université Libre de Bruxelles, Brussels, Belgium
L. J. Nevay, W. Shields, S. T. Boogert, Royal Holloway, University of London, Egham, UK
[1]also at CERN, Meyrin, Switzerland

Abstract

Hadron therapy centres are evolving towards reduced-footprint layouts, often featuring a single treatment room. The evaluation of beam properties, radiation protection quantities, and concrete shielding activation via numerical simulations poses new challenges that can be tackled using the numerical beam transport and Monte-Carlo code Beam Delivery Simulation (BDSIM), allowing a seamless simulation of the dynamics as a whole. Specific developments have been carried out in BDSIM to advance its efficiency toward such applications, and a detailed 4D Monte-Carlo scoring mechanism has been implemented. It produces tallies such as the spatial-energy differential fluence in arbitrary scoring meshes. The feature makes use of the generic `boost::histogram` library and allows an event-by-event serialisation and storage in the ROOT data format. The `pyg4ometry` library is extended to improve the visualisation of critical features such as the complex geometries of BDSIM models, the beam tracks, and the scored quantities. Data are converted from Geant4 and ROOT to a 3D visualisation using the VTK framework. These features are applied to a complete IBA Proteus One model.

INTRODUCTION

Clinical findings have shown that the efficiency of proton therapy can be greater than X-ray radiotherapy for specific types of tumours, such as for paediatric cancers, skull-based, sino-nasal malignancies and brain tumours [1]. The specific features of protons dose deposition into matter, well known as "Bragg peaks", allow for a more precise dose deposition during treatments and should cause less radiation-induced cancers by reducing dramatically the radiation exposure of normal tissue [1].

However, proton therapy requires more complex and advanced technologies than classical radiotherapy and therefore leads to higher construction costs for the complete systems. Proton therapy centres were initially built with multiple treatments rooms sharing one proton beam. Their construction was therefore limited to large medical centres able to cope with the larger costs. Consequently, the number of proton therapy centres has always been lower than the number of conventional radiotherapy centres resulting in fewer studies in proton therapy than in radiotherapy. The proton therapy centres costs combined with the lack of clinical studies have therefore hindered the evolution of proton therapy in comparison to traditional radiotherapy [2]. The development of the future proton therapy centres aims to reduce the construction cost by decreasing the proton therapy centre size and by proposing single-room designs featuring compact gantries [3].

The size reduction of proton therapy centres coupled with the increase of research efforts must be taken into account in the design process of future proton therapy centres. One consequence is the increase of radiation to the system itself (accelerator, beamline, gantry and concrete shielding), leading to a higher overall activation. This must be taken into account, as the decommissioning of activated materials contributes to a large fraction of the total cost of the system. Initial studies on new types of concrete whose composition decreases the final quantity of radioactive waste after the typical proton therapy centre lifespan of 20 years have been performed [4–6]. Detailed simulations regarding the overall activation must be realised.

New methods have been developed to answer the new challenges that these ongoing studies pose for the numerical simulations that evaluate the beam properties, the radiation protection quantities, and the concrete shielding activation. Indeed, the reduction in size of the proton therapy centres coupled with the increase of research experiments induces inevitably a higher mean irradiation rate. The precision required from the simulations is also increased: under greater and longer fluxes the radiation protection and environmental limits are more quickly reached. These challenges can be tackled by using the numerical beam transport and Monte-Carlo code Beam Delivery SIMulation (BDSIM) [7], a Geant4-based particle tracking code [8, 9], which allows a seamless simulation of the beam dynamics as a whole. The use of BDSIM for proton therapy applications is discussed in detail in [10].

BDSIM allows 3D scoring maps and activation computation using the Geant4 physics libraries. The possibility to compare with other physics libraries and computational methods is key for further studies, in particular for the computation of shielding activation. Simulations results data are inherently complex and 3D visualisations would greatly aid in their understanding. This contribution details new developments that have been carried out in BDSIM and its associated tools and libraries to advance its capabilities toward complete proton therapy system simulations.

* eliott.ramoisiaux@ulb.be

ISBN: 978-3-95450-214-1 ISSN: 2673-5490 doi:10.18429/JACoW-IPAC2021-MOPAB416

3D VISUALISATION CONVERSION

The first new development is an improved 3D visualisation of the BDSIM model and simulation results. A Python-based toolbox has been developed to provide conversion mechanisms, from the Geant4 geometry format and ROOT data [11] to a 3D visualisation using the VTK framework [12]. It supports the complex geometries used by the BDSIM models, the transported beam tracks, and the scored quantities. An additional feature is the possibility to directly import the converted files into Paraview [13] and save all the exported model elements into a Paraview state file (`.pvsm`) with their correct positioning and colours. Paraview is based on VTK but provides a higher-level interface to visualise data structures, as opposed to primitive shapes and objects in VTK. The model elements colour can be defined either following the element materials or following the element type. In this latter case, the same colour is taken as in the BDSIM model (*e.g.* quadrupoles in red, dipoles in blue, etc.). The toolbox has been implemented in `pyg4ometry` [14], a Python library allowing the conversion to and from different geometry description formats.

Figure 1 shows the IBA Proteus One with its associated concrete shielding and the primary proton beam, exported in the VTK format, and visualised in Paraview. The colours of the majority of the beamline elements have been chosen to follow the BDSIM colour code, apart from the cyclotron, the degrader which is a rotating wheel with blocks of different thicknesses of three varied materials (Aluminium, Graphite and Beryllium) [15], and the last bending magnet (B3G). Those elements have their complex geometries exported from unique GDML files (the Geant4 geometry persistency format [16]) with their colour either manually specified as for the S2C2 and B3G or chosen to follow its composite material colours as for the degrader. The concrete shielding is represented with two distinct colours to highlight the presence of two different types of concrete in the shielding walls. A complete description of the model can be found in [10].

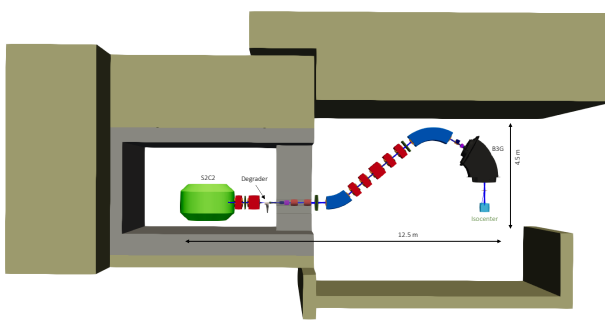

Figure 1: Paraview model of the IBA Proteus One, its shielding and its proton beam exported from BDSIM in VTK format.

The shielding activation finds its origin in the secondary neutrons nuclear reactions (capture or spallation) inside the concrete walls. Their production is induced by the collisions of the primary beam with the degrader. These interactions are meant to define the mean beam energy during treatments. The secondary neutron fluxes are extracted from the BDSIM simulations using dedicated python code based on `pybdsim` [17] using the `uproot` [18] and the VTK libraries. The data are then integrated into Paraview by conversion of the resulting ROOT histograms into VTK format. Figure 2 represents the result of such an extraction: the secondary neutron fluence scoring data are visualised inside the Paraview model. Paraview provides a large number of ways of visualising the histograms data. The "surface" visualisation has been chosen for the back wall and the floor while the "volume" visualisation has been chosen for the walls linking the vault where the accelerator lies and the treatment room. The 3D observation of the secondary fluxes results shows hotspots in the area around the degrader which would typically be zones of interest for a thorough activation computation. The methodology is described in Fig. 3.

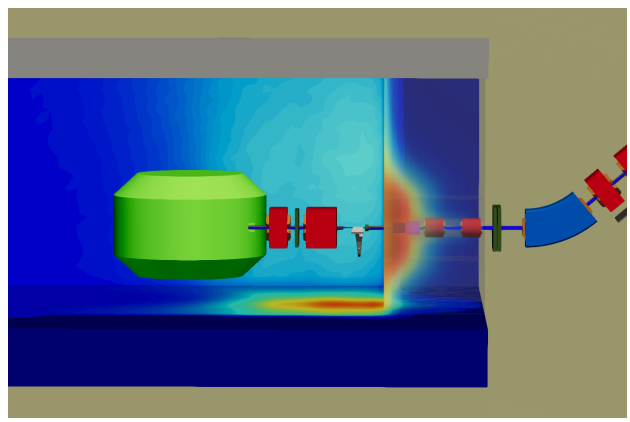

Figure 2: Paraview model of the IBA Proteus One, its shielding, its primary proton beam in blue and the secondary neutron fluence exported from BDSIM in VTK format. The 3D representation of the secondary neutrons fluence scoring data is using a colormap to highlight the fluence hotspots.

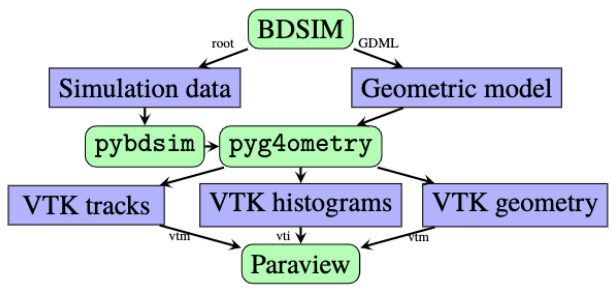

Figure 3: Diagram of the 3D visualisation conversion methodology.

In addition to displaying the BDSIM results in a 3D model, a great number of other visualisation tools are available to optimise the way the results are presented such as the possibility to directly include DICOM files to visualise the patient scans slice by slice or with a volume rendering. Figure 4 illustrates the added value of using Paraview as viewer for BDSIM with the visualisation of two protons beams interacting in a phantom.

ISBN: 978-3-95450-214-1 ISSN: 2673-5490 doi:10.18429/JACoW-IPAC2021-MOPAB416

Figure 4: Paraview visualisation of two proton beams interacting with a phantom extracted from a DICOM file. The phantom is obtained from the combination of CT scans slices saved in the DICOM file. Paraview visualisation settings have been used to obtain the resulting figure: the back of the phantom is visualised with the "surface" style while the patient's bone structure follows a volumetric rendering.

4D MONTE-CARLO SCORING

The second new development is the capability to tally the energy differential particle fluence in BDSIM simulations. More precise activation results can be obtained by coupling the Monte-Carlo code BDSIM with the code system and library database FISPACT-II [19]. FISPACT-II allows a thorough calculation of the shielding activation in the form of inventories and radiological output computations. As input information, FISPACT-II requires the differential particles fluxes at any point of interest and such with a specific energy meshing following some predefined group structures (ex: CCFE-709, UKAEA-1102, etc.). The new feature is a detailed 4D Monte-Carlo scoring mechanism that produces tallies such as spatial-energy differential fluence in arbitrary scoring meshes. This feature makes use of the generic `boost::histogram` library [20] and allows an event-by-event serialisation and storage in the ROOT data format. The arbitrary N-dimension histogram class provided by ROOT has not been chosen as it does not permit uneven binning (*e.g.* logarithmic or user-defined) as required to cover many orders of magnitude in energy with multiple discontinuities in the spectra or simply to be compatible with auxiliary programs.

As an illustration of the new 4D scoring feature, the differential fluence has been computed for the right-hand side wall of the degrader where the secondary particle fluence has been shown to be important in Fig. 2. The 4D scoring has been realised following the CCFE-709 energy group structure binning of the FISPACT-II nuclear data libraries and with four bins along with the wall thickness. Importance sampling has been used in the BDSIM simulation to obtain similar statistics at all depths. On Fig. 5, the thermal spectrum of the neutrons having reached equilibrium with the degrader atoms can be observed at low energy while abrupt changes in the differential flux can be observed at around 10 MeV as spallation reaction becomes more important than capture around this energy level [21].

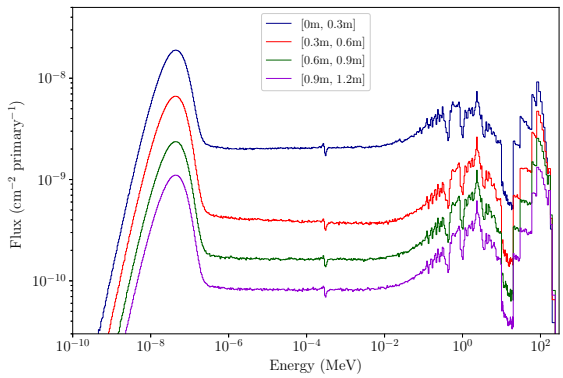

Figure 5: Representation of the differential secondary neutron fluence extracted from the wall on the right of the degrader using the new 4D scoring feature. The energy binning follows the CCFE-709 energy group structure and has been taken from 10^{-10} MeV to 250 MeV. Each colour represents the neutron differential fluence at different depths in the walls.

The new 4D scoring feature can also find use in other kinds of study such as in $H^*(10)$ ambient dose equivalent maps computations as presented in [10]. Indeed, $H^*(10)$, defined as the dose produced in a 30 cm diameter tissue-equivalent sphere of unit density at a depth of 10 mm on the radius opposing the direction of the irradiation field [22], is computed by making the product between the differential particle fluence ϕ (cm^{-2}) and the fluence-to-ambient dose equivalent conversion coefficients h_{10} (Sv × cm^{-2}). Those h_{10} conversion coefficients can be found on [23]. The ambient dose expression is then $H^*(10) = \sum \phi(E, \text{particle}) \times h_{10}(E, \text{particle})$. The differential fluxes extracted by the new 4D scoring can therefore easily compute such kinds of radiological quantities based on one scorer without having to use each of the BDSIM scorers associated with these specific quantities. Computing another radiological quantity would only require conversion coefficients and no other simulation.

CONCLUSION AND OUTLOOK

Two novel features developed to improve the capabilities of BDSIM for proton therapy applications have been presented in this paper and illustrated with simulations using the complete IBA Proteus One model. The 3D visualisation using Paraview greatly improves the visualisation of key simulation results. The 4D Monte-Carlo scoring allows the coupling of BDSIM with other codes, such as FISPACT-II, to achieve more precise overall studies.

REFERENCES

[1] M. Durante, R. Orechhia, and J. S. Loeffler, "Charged-particle therapy in cancer: clinical uses and future perspectives", *Nature Reviews Clinical Oncology*, vol. 14, no. 8, pp. 483–495, Aug. 2017. doi:10.1038/nrclinonc.2017.30

ISBN: 978-3-95450-214-1 ISSN: 2673-5490 doi:10.18429/JACoW-IPAC2021-MOPAB416

[2] R. Mohan and D. Grosshans, "Proton therapy – Present and future", *Advanced Drug Delivery Reviews*, vol. 109, pp. 26–44, Jan. 2017. doi:10.1016/j.addr.2016.11.006

[3] J. B. Farr, J. B. Flanz, A. Gerbershagen, and M. F. Moyers, "New horizons in particle therapy systems", *Medical Physics*, vol. 45, no. 11, pp. e953–e983, 2018. doi:10.1002/mp.13193

[4] F. Stichelbaut, "Development of low-activation concrete for the ProteusONE system", IBA, Louvain-La-Neuve, Belgium, Rep. 50897, 2016.

[5] R. Tesse, "Quantitative methods to evaluate the radioprotection and shielding activation impacts of industrial and medical applications using particle accelerators", Ph.D. thesis, Free University of Brussels, Brussels, Belgium, 2018.

[6] R. Tesse *et al.*, "Simulations of the Activation of a Proton Therapy Facility Using a Complete Beamline Model With BDSIM", in *Proc. 10th Int. Particle Accelerator Conf. (IPAC'19)*, Melbourne, Australia, May 2019, pp. 4176-4179. doi:10.18429/JACoW-IPAC2019-THPTS031

[7] L. J. Nevay *et al.*, "BDSIM: An accelerator tracking code with particle-matter interactions", *Computer Physics Communications*, vol. 252, p. 107200, Jul. 2020. doi:10.1016/j.cpc.2020.107200

[8] S. Agostinelli *et al.*, "Geant4 — a simulation toolkit", *Nuclear Instruments and Methods in Physics Research Section A: Accelerators, Spectrometers, Detectors and Associated Equipment*, vol. 506, no. 3, pp. 250–303, Jul. 2003. doi:10.1016/S0168-9002(03)01368-8

[9] J. Allison *et al.*, "Recent developments in Geant4", *Nuclear Instruments and Methods in Physics Research Section A: Accelerators, Spectrometers, Detectors and Associated Equipment*, vol. 835, pp. 186–225, Nov. 2016. doi:10.1016/j.nima.2016.06.125

[10] C. Hernalsteens *et al.*, "A novel approach to seamless simulations of compact hadron therapy systems for self-consistent evaluation of dosimetric and radiation protection quantities", *European Physics Letters*, vol. 132, no. 5, p. 50004, Dec. 2020. doi:10.1209/0295-5075/132/50004

[11] R. Brun and F. Rademakers, "ROOT — an object oriented data analysis framework", *Nuclear Instruments and Methods in Physics Research Section A: Accelerators, Spectrometers, Detectors and Associated Equipment*, vol. 389, no. 1–2, pp. 81–86, Apr. 1997. doi:10.1016/S0168-9002(97)00048-X

[12] W. Schroeder, K. Martin, and B. Lorensen, *The Visualization Toolkit*, 4th Ed., New York, USA: Kitware, 2006.

[13] J. Arhens, B. Geveci, and C. Law, "ParaView: An End-User Tool for Large-Data Visualization", in *Visualization Handbook*, C. D. Hansen and C. R. Johnson, Eds., Oxford, UK: Elsevier, 2005, pp. 717-732.

[14] S. T. Boogert, A. Abramov, L. J. Nevay, W. Shields, and S. D. Walker, "PYG4OMETRY: a Python library for the creation of Monte Carlo radiation transport physical geometries", 2021. arXiv:2010.01109

[15] R. Tesse, A. Dubus, N. Pauly, C. Hernalsteens, W. Kleeven, and F. Stichelbaut, "Numerical simulations to evaluate and compare the performances of existing and novel degrader materials for proton therapy", *Journal of Physics: Conference Series*, vol. 1067, p. 092001, Sep. 2018. doi:10.1088/1742-6596/1067/9/092001

[16] R. Chytracek, J. Mccormick, W. Pokorski, and G. Santin, "Geometry description markup language for physics simulation and analysis applications", *IEEE Transactions on Nuclear Science*, vol. 53, no. 5, pp. 2892–2896, Oct. 2006. doi:10.1109/TNS.2006.881062

[17] L. J. Nevay *et al.*, Pybdsim, http://www.pp.rhul.ac.uk/bdsim/pybdsim/.

[18] J. Pivarski *et al.*, "uproot4", 2021. doi:10.5281/zenodo.4680970

[19] J.-Ch. Sublet, J. W. Eastwood, J. G. Morgan, M. R. Gilbert, M. Fleming, and W. Arter, "FISPACT-II: An advanced simulation system for activation, transmutation and material modelling", *Nuclear Data Sheets*, vol. 139, pp. 77–137, 2017. doi:10.1016/j.nds.2017.01.002

[20] Boost C++ Libraries, http://www.boost.org/.

[21] R. Tesse, F. Stichelbaut, N. Pauly, A. Dubus, and J. Derrien, "GEANT4 benchmark with MCNPX and PHITS for activation of concrete", *Nuclear Instruments and Methods in Physics Research Section B: Beam Interactions with Materials and Atoms*, vol. 416, pp. 68–72, Feb. 2018. doi:10.1016/j.nimb.2017.12.006

[22] M. Pelliccioni, "Overview of Fluence-to-Effective Dose and Fluence-to-Ambient Dose Equivalent Conversion Coefficients for High Energy Radiation Calculated Using the FLUKA Code", *Radiation Protection Dosimetry*, vol. 88, no. 4, pp. 279–297, Apr. 2000. doi:10.1093/oxfordjournals.rpd.a033046

[23] ULB-Metronu bdsim-datafiles, https://github.com/ULB-Metronu/bdsim-datafiles